Development of a model for the prediction of the fretting fatigue regimes

T.E. Matikas
Greek Atomic Energy Commission, P.O. Box 60092, 15310 Ag. Paraskevi, Athens, Greece

P.D. Nicolaou
Silver and Baryte Ores Mining Co., S.A., GR 10672, Athens, Greece

The parameters that govern the life of metallic materials under conditions of fretting fatigue may be divided into two broad categories. The first category concerns the material properties (e.g., yield strength, elastic modulus, and surface roughness) while the second concerns the externally imposed loading conditions and contact geometry. The two in-contact materials may either stick, slip, or stick-slip (i.e., there is a slip and a stick region on their interface) against each other. It has been shown that the fatigue life reduction is highest under partial slip. The objective of the present research effort is to develop a model that enables the prediction of the particular fretting fatigue regime (i.e., slip, stick, or mixed). The parameters that affect the fretting fatigue life of metallic components were identified and integrated into a model, which allows the prediction of the interfacial contact conditions. The model was first used to identify the sensitivity of the fretting fatigue regimes upon the materials and external, and geometrical parameters. Experimental results concerned with the fatigue life were plotted on the fretting maps; the fretting fatigue regimes indicated by the latter enabled the interpretation of the experimental data.

I. INTRODUCTION

Fretting is defined as the small amplitude oscillatory motion between two components that are in contact. When the relative movement is the consequence of a cyclic load, which is applied to one of the components, the process is then termed fretting fatigue. Fretting fatigue is a material damage process that involves the synergistic action of three discrete mechanisms: wear, corrosion, and fatigue. Any nominally clamped components that are subjected to transient variations or oscillatory loads are susceptible to fretting damage. Reports of fretting damage span a range of tribological systems as diverse as riveted lap joints, ball bearings, orthopedic implants, turbine blades, and steel ropes, among others.[1–3]

Fretting fatigue is a surface phenomenon. Unlike plain fatigue, where the formation phase of crack development is normally associated with the presence of some pre-existing macroscopic discontinuities or free formation of a crack from some surface irregularity, fretting fatigue is essentially a process involving the interaction between two bodies. The role of fretting on the fatigue life is confined to the formation and growth of a crack to a length, which is comparable with the characteristic dimension of the contact; at this point the influence of the contact stress field itself is essentially diminished and the crack might equally be one associated with plain fatigue. The fretting process itself is controlled by the bulk geometry of the contacting bodies, their surface finish, the physical and mechanical properties of the two bodies (in particular their elastic properties, yield strength, thermal conductivity, and thermal diffusivity) and the applied loading history.[4–6]

Depending on the external loading, the geometrical parameters, and the material properties, two surfaces in contact may either slip against each other, stick, or there may be a region of stick and a region of slip between them. The nature of the contact conditions defines the particular regime of fretting fatigue, i.e., slip, stick, or the mixed (stick-slip). The damage mechanism, and thus the life reduction, varies among the different contact conditions. In particular, there is essentially no damage between "sticking" surfaces, material wear and particle detachment occurs between two "slipping" surfaces, while for surfaces whose contact is within the mixed regime the damage occurs by the formation of cracks.[7,8] While the life reduction is minimal in the slip and stick regimes, components within the mixed regime experience significant life reductions. In particular, strength reduction factors (defined as the fatigue strength of a material under plain fatigue to the strength under fretting fatigue) in the order of three are not uncommon for

fretting fatigue systems in the mixed regime.[6,9] The experimental work of Nishioka *et al.*,[10] Nishioka and Hirakawa,[11] and Gaul and Duquette[12] has demonstrated that the fretting fatigue life decreases with increasing the slip amplitude (i.e., in the transition from the stick to the mixed regime). This life decrease occurs up to certain amplitude where the fatigue life starts to increase again (transition from the mixed to the slip regime). Similar trends were also obtained from other experimental studies.[13,14] It is evident that for a given material system the slip amplitude depends on the normal stress, the maximum cyclic stress, and the contact geometry. In addition, it should be mentioned that the slip length is of great importance within the mixed regime because it determines the ratio of the slip to the stick length of the contact area. Under most contact geometries, crack formation occurs at the slip/stick boundary; it has been shown that the stress concentration is much greater when the stick region is narrow and thus the possibility of crack formation (and hence the life reduction) is much higher.[1,15]

These arguments imply that the *a priori* knowledge of the particular fretting fatigue regime is very important in predicting (or at least estimating) the life reduction of a component. To this end, the present work is focused on the development of fretting maps, i.e., diagrams that show the relevant regimes in two variables (normal and maximum cyclic stress), with regime boundaries representing critical values for the transition from one regime to another. Because the life of a component is related to the particular fretting fatigue regime, a fretting map of a tribosystem can facilitate the choice of the operating (e.g., loading) parameters such that fretting problems are alleviated.

II. EXISTING EXPERIMENTAL OBSERVATIONS

In this section, experimental data earlier published in the literature are summarized. These data describe the fretting fatigue phenomenon through the adhesion between two surfaces, the formation and breakup of local microwelds. This short review is necessary in order to ensure that the model, which is developed in Sec. III, is realistic and relies on actual experimental observations.

When a normal load is applied between two components in contact local asperity microwelding is taking place. In the stick regime the bulk displacement of the vibrating specimen is completely accommodated by elastic and plastic shear near the interface material, with no relative slip taking place at the interface. As observed during fretting fatigue of niobium specimens,[16] the interface is maintained under stick contact conditions by the adhesively joined (microwelded) asperities, which due to the fretting motion are sheared back and forth by plastic deformation. Between the individual asperity

contact points/areas no visible damage is occurring and fretting wear is not produced. On the other hand, in the slip regime, the microwelds between asperities are breaking up and each individual asperity makes contact with several asperities of the opposite surface. Sliding wear scars are obtained under slip conditions. The mixed (slip-stick) regime can be described by a combination of the observations given above, i.e., a region resembling the stick regime and another region resembling the slip regime.

Regarding the size/location of the slip and stick regions in the mixed regime, recent developments[17–19] have shown that in a contact problem with constant normal load/stress, the slip and the stick zones remain the same as "activated" during the normal loading process. This indicates that the fretting pattern is "decided" before the application of the cyclic stress. This pattern depends solely on the geometry of the contacting surfaces and on the magnitude of the normal applied stress. The validity of this statement was enhanced by the wavelet analysis of Frantziskonis *et al.*[19] on the slip and stick regions of fretted specimens. Their work showed that these surfaces, represented by the wavelet coefficients from the transform of profilometry images, are optically similar; in other words the fretting pattern is closely related to the surface features of the as-received condition.

III. MODEL DEVELOPMENT

The experimental observations and the numerical analyses presented in Sec. II are used to formulate a model that enables the prediction of the particular fretting fatigue regime as a function of the applied stresses (normal and maximum cyclic), the properties of the materials, and the surface conditions.

Assume first two flat materials in contact with each other, as shown in Fig. 1(a). Using standard fretting fatigue terminology,[20] Material 1 is termed the specimen, while Material 2 is termed the fretting pad. For the sake of simplicity, it is assumed that both the specimen and the pad are of the same material. The model comprises two distinct stages. In the first stage the application of the normal stress leads to yielding and microwelding of the surface asperities. In the second stage the cohesion between the two surfaces is breaking up because the application of the cyclic stress generates shear stresses in the interface of the two components.

A. Cohesion of surfaces/microwelding

The term microwelding defines the formation of a solid bond between two asperities of the opposite surfaces.[21] Because no surface is perfectly flat, these bonds do not form all along the contact plane; rather they are formed locally, where two asperities come into contact and deform plastically due to the application of the normal stress.
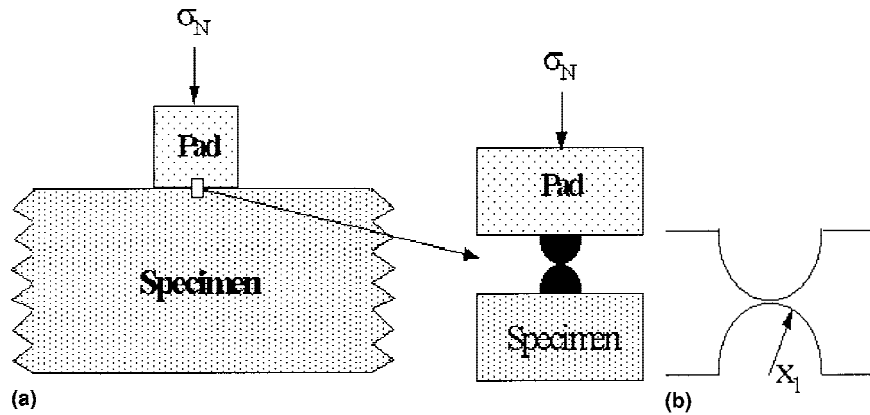
FIG. 1. Schematic diagram showing (a) two bodies in contact and (b) the local asperity contact between the two bodies.

Consider the schematic of Fig. 1(a), which shows the contact of two rough surfaces under a normal stress σ_N. A unit cell, which contains one asperity from each surface, is selected to analyze the deformation and bond formation process [Fig. 1(b)]. It is assumed that all asperities are semispherical and they are under point contact prior to the application of the normal stress, σ_N. Instantaneously with the application of σ_N, the flow stress of the materials may be exceeded and a neck between the two asperities will be formed [Fig. 1(c)]. By neglecting elastic deformation and assuming a perfectly plastic material with a constant flow stress σ_y, the equilibrium neck size can be determined by resource to slip-line theory,[22] i.e., plastic deformation under plane-strain conditions.

From slip-line theory it is calculated that the compressive stress (P_A) required to produce a contact neck radius α in a perfectly plastic material is[23]

$$P_A = \frac{\sigma_y}{2}\left[2 + \pi\left(1 - \frac{\alpha}{x_1}\right)\right] \quad , \tag{1}$$

in which x_1 denotes the initial radius of curvature of the asperities as shown in Fig. 1(b). In the beginning of the process, $\alpha = 0$, then the stress P_A is given by

$$P_A = \frac{\sigma_y}{2}(2 + \pi) \quad . \tag{2}$$

As the neck grows, the angle at which the two asperities meet, increases from zero toward $\pi/2$. Thus according to Eq. (1) the apparent "hardness" of the asperities decreases. At a given contact radius α the condition for sustaining yielding is

$$P_A > \frac{\sigma_y}{2}\left[2 + \pi\left(1 - \frac{\alpha}{x_1}\right)\right] \quad . \tag{3}$$

Notice that during the process two counteracting effects are influencing the neck development: (i) the decrease of the "apparent" asperity hardness, with the increase of α,

and (ii) the decrease of the compressive stress per asperity contact P_A because of the increase in the contact area (i.e., bond area).

The total *actual* contact area can be determined by taking into account the material flow stress, the externally applied normal stress, and the surface roughness (i.e., number of asperities per unit area). Assume that all asperities are of the same height and that they are uniformly distributed in the two (specimen and pad) surfaces. If A is the area of the pad (which equals the nominal contact area), then the total number of asperities N in area A is given by the following equation:

$$N = A/L^2 \quad , \tag{4}$$

where L denotes the spacing between the asperities. In addition, the compressive stress per asperity is given by

$$P_A = \sigma_N/N \quad or \quad P_A = \sigma_N L^2/A \quad . \tag{5}$$

For a given normal stress the neck radius α is determined from Eqs. (1) and (5). The total, actual bond area A_b is equal to the contact area per asperity ($= \pi\alpha^2$) multiplied by the total number of asperities in A, i.e.,

$$A_b = (1/L^2) \pi \alpha^2 \quad . \tag{6}$$

B. Breaking of cohesion: Slip of surfaces

The second part of the model deals with the breakup of cohesion by shearing the interfacial asperity microwelds between the two bodies. Shear stresses are developed in the specimen and the pads as soon as a stress is imposed in the longitudinal direction on one of the components (in this case the specimen). Because the total *actual* welded area is only a fraction of the *apparent* (macroscopic) area A, it is then expected that failure will occur at the specimen/pad interface.

Breaking of the cohesion between the two materials does not always occur, especially when the maximum cyclic stress σ_{max} is low; in this case the two bodies may stick to each other. On the other hand, a high

σ_{max} can lead to total slip between the two components. In addition, there might be a combination of the above, i.e., an area of stick and an area of slip respectively. The particular interface contact conditions define the fretting fatigue regime and they are dependent upon both the maximum cyclic stress σ_{max} and the normal stress σ_N.

The frictional resistance (defined as the minimum tangential force necessary to initiate sliding) between the two surfaces is determined by the sum of a shearing and a ploughing component. In the case of fretting fatigue where the displacements are quite low the ploughing term is insignificant with respect to the shearing term and it will be neglected in the subsequent analysis.[24] Because asperities have yielded the shearing term, which is the resistance of the junctions so formed by the plastic yielding, requires that the junctions must be broken completely before the rider (fretting pad) can move over the specimen. If τ is the shear strength of the metal components, the (shearing) stress S required for sliding is given by the following relationship:

$$S = (A_b/A)\,\tau \quad . \tag{7}$$

Consider the specimen/pad geometry shown in Fig. 2. The pad is located at the center of the specimen and has a width of $2w$ and a normal stress σ_N is imposed on it. A cyclic stress σ ranging from σ_{min} to σ_{max} is applied on the specimen.

The nature of the fretting fatigue regime (i.e., stick, slip, or partial slip) depends on the following two conditions: (i) the magnitude of the shear stress at the interface and (ii) the local, relative, displacement between the two bodies.

Regarding the first condition, if the interfacial shear stress is less than S then no sliding will occur. However, as is indicated by the second condition, the local specimen displacement against the stationary rider should be high enough so as two bonded asperities located at a distance x from the specimen's center separate totally from one another. The elastic displacement varies during a fatigue cycle and it reaches its maximum value at σ_{max}. There are two factors which oppose the elastic deformation of the specimen: (i) the resistance of the specimen to

elastic deformation and (ii) the resistance of the microbonds (formed after the application of the normal stress) to yielding. By taking into account these two effects, one can arrive to the following equation:

$$d_x = \frac{[\sigma_{max} - \tau(A_b/A_{sp})]}{E}\, x \quad . \tag{8}$$

Equation (8) describes the specimen's displacement (d_x) at a distance x from its center, while A_{sp} is the specimen's cross-sectional area, and E the elastic modulus of the specimen. The distance x varies between zero and half of the pad's length w. A schematic of asperity separation due to the relative movement between the two bodies is shown in Fig. 3. If d_w is the specimen's displacement at $x = w$, then the different fretting fatigue regimes are determined as

(i) Stick:	$d_w < 2\,\alpha$,	(9)
(ii) Slip or Partial Slip:	$d_w > 2\,\alpha$.	(10)

It should be mentioned here that the slip regime cannot occur for the geometrical conditions used here, i.e., the pad located exactly at the center of the specimen where the displacement is zero.[25] However, in order to account for actual situations, where a small shift of the pad's and specimen's centers is possible, full slip is assumed to occur if the following condition is satisfied:

$$\text{(iii) Slip:} \qquad d_{x_{in}} > 2\,\alpha \quad , \tag{11}$$

where $d_{x_{in}}$ denotes the displacement at a very small, compared to w, distance x_{in} from the specimen's center.

In summarizing this section, it should be noted that general relationships were developed and they can be applied to any system for predicting the particular fretting fatigue regime.

IV. MODEL PREDICTIONS: SENSITIVITY ANALYSIS

A parametric study of the effect of the material's properties, surface conditions, and pad size on the boundaries of the fretting fatigue regimes is conducted in this section
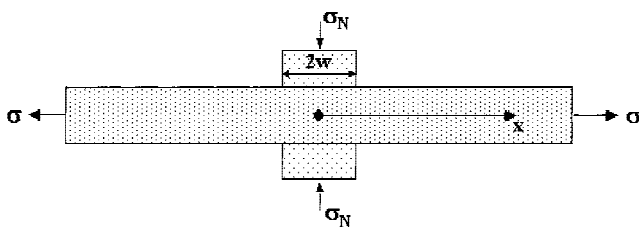

FIG. 2. Schematic diagram of a specimen undergoing a cyclic stress, with a second body of width $2w$ being in contact with it under a normal load F.
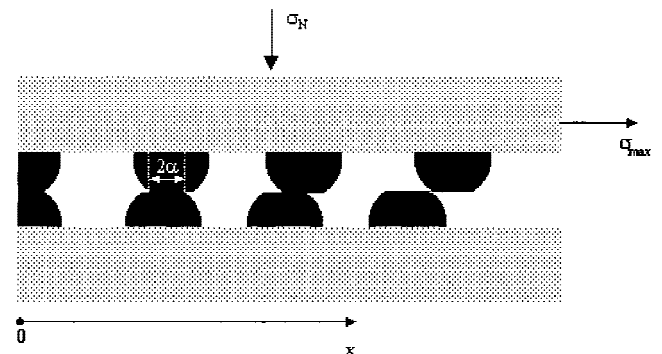

FIG. 3. Relative motion of the asperities because of the cyclic stress imposed on the specimen.

of the article. For the sake of generality, the normal as well as the maximum cyclic stress σ_N and σ_{max} are normalized to the yield strength of the fretting fatigued materials. A fretting map, based on Eqs. (1) to (11), is shown in Fig. 4, where normal is plotted against the maximum cyclic stress. This map corresponds to the following parameters: $\sigma_y/E = 8.2 \times 10^{-3}$, $A/A_{sp} = 0.5$, $w = 5$ mm, $L = 60$ μm, and $x_1 = 20$ μm.

The dashed line A on the graph represents the interfacial shearing stress S required for sliding [Eq. (7)]. On the left hand side of line A, the interfacial shear stress developed at the pad/specimen interface is not high enough to break the cohesion between the two materials; thus no sliding between the two will occur. The opposite holds true for the right-hand side of line A. The two solid lines B and C represent the relationships (9) and (11) respectively. For the parameters of w, E, L, A, A_{sp}, and x_1 used in the model to construct this map, it is seen that the stress σ_{max} required to displace the pad against the specimen enough for slip to occur is larger than the shearing stress S; hence the boundaries of the fretting fatigue regimes are determined only by the relationships (9) and (11). Qualitatively the specimen/pad interfacial contact conditions can be described as follows: stick, high σ_N–low σ_{max}; slip, low σ_N–high σ_{max}; mixed, intermediate σ_N–intermediate σ_{max}.

Notice that this qualitative determination of the fretting fatigue regimes is in agreement with those determined from actual experimental measurements.[26]

As mentioned above, the location of the fretting fatigue regime boundaries on the σ_N–σ_{max} graphs are dependent on the material properties, surface finish,

and contact geometry (for the flat pads assumed here, the contact geometry effect is limited to the effect of the contact length). Because of the symmetry of the contact geometry (i.e., the center of the surface of the pad coincides with the center of the specimen), our attention is focused on the stick/mixed regime boundary. From the fretting fatigue life standpoint, it is desirable that this boundary is "shifted" toward higher σ_{max} values (for a constant σ_N); thus the interfacial contact conditions remain in the stick regime for a wider range of σ_{max}–σ_N combinations.

The effect of the specimen's elastic modulus is shown in Fig. 5. It is seen that for a constant normal stress, the stick/mixed regime boundary is shifting toward higher σ_{max} values as the elastic modulus increases. Thus, a stiffer material possibly suffers less damage under conditions of fretting fatigue. Figure 6 represents an example of a fretting map, in which the effect of the pad length w on the location of the stick/mixed boundary is identified. It can be observed that when the pad length increases it is easier for the mixed regime to prevail. Regarding the surface roughness, which is expressed as asperity spacing and height, Figs. 7(a) and 7(b) shows examples of such a fretting map. With regard to the asperity height, it was observed that the results are not very sensitive upon x_1. This observation can be attributed to the fact that the contact radius between two deformed asperities does not vary significantly with x_1 for the range of the normal stresses used. On the other hand, Fig. 7(b) reveals that as the asperity spacing increases σ_{max} should be increased for slip to occur. This result can be attributed to the fact
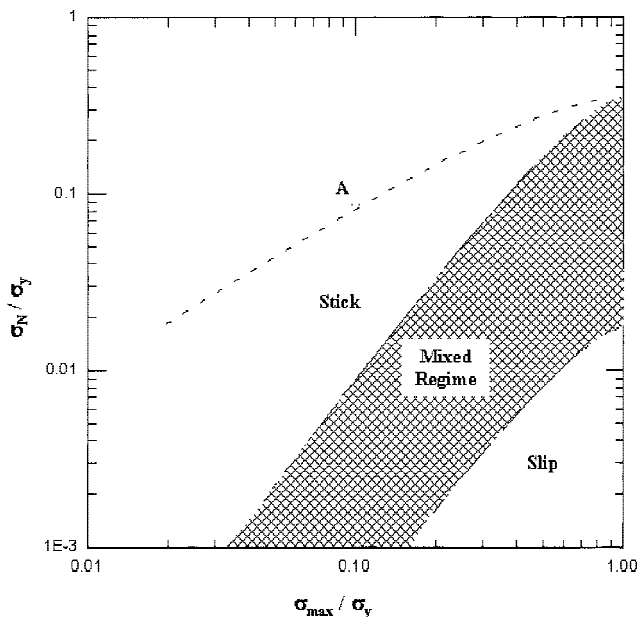

FIG. 4. Prediction of the different fretting fatigue regimes as a function of the normal and maximum cyclic stress.
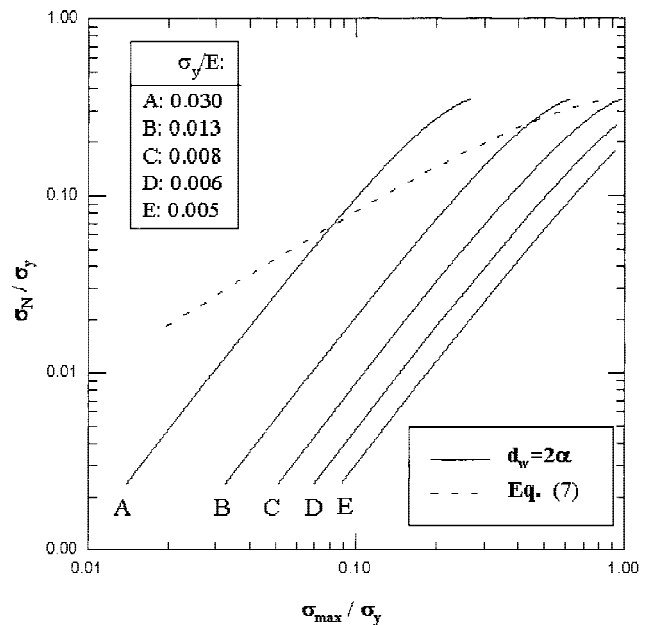

FIG. 5. Sensitivity of the fretting fatigue regimes upon the elastic modulus of the specimen.
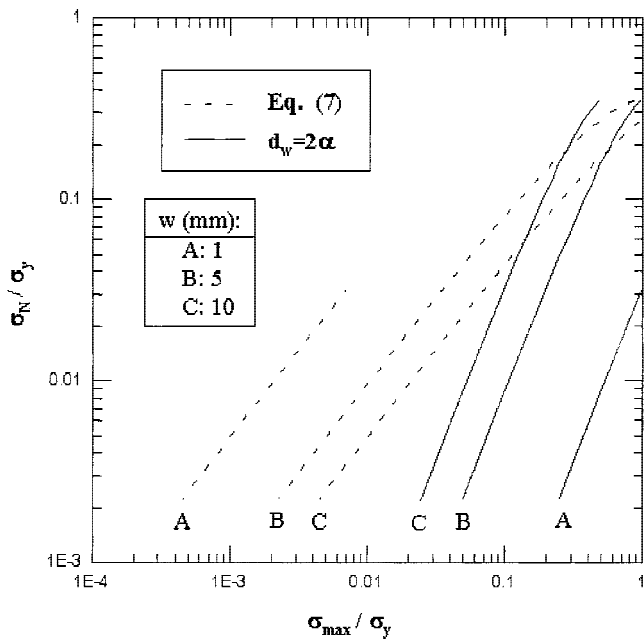
FIG. 6. Effect of the pad size on the location of the fretting fatigue regimes.

that as L increases, the stress per contact increases too, the final contact radius is higher, and thus the axial (specimen) displacement should be increased in order to slide one material against the other.

In summary of this parametric analysis, it can be deduced that the interfacial contact conditions are sensitive to the material properties, contact geometry, and surface conditions.

V. FRETTING MAPS OF TI–6AL–4V ALLOYS: INTERPRETATION OF FRETTING FATIGUE LIFE

Earlier published experimental data[27] concerned with the fretting fatigue life of a Ti–6Al–4V alloy can be interpreted with the aid of fretting maps. The fretting map for the Ti–6Al–4V alloy for the particular material contact conditions is constructed first, then the fretting fatigue data are plotted on the map and the fretting fatigue lives are interpreted according to the particular regime they belong to. In order to construct the fretting map for this case, the materials properties, the contact characteristics, and surface conditions must be known. The first two are given in Ref. 27. On the other hand, the other important input parameter for the model, surface conditions expressed by the asperity spacing and height, was not reported; yet only the particular surface preparation technique is given. In order to overcome this obstacle, we conducted a similar surface preparation procedure on the Ti–6Al–4V specimens and pads of the same microstructure and the surface asperity height and spacing were determined using white light interference
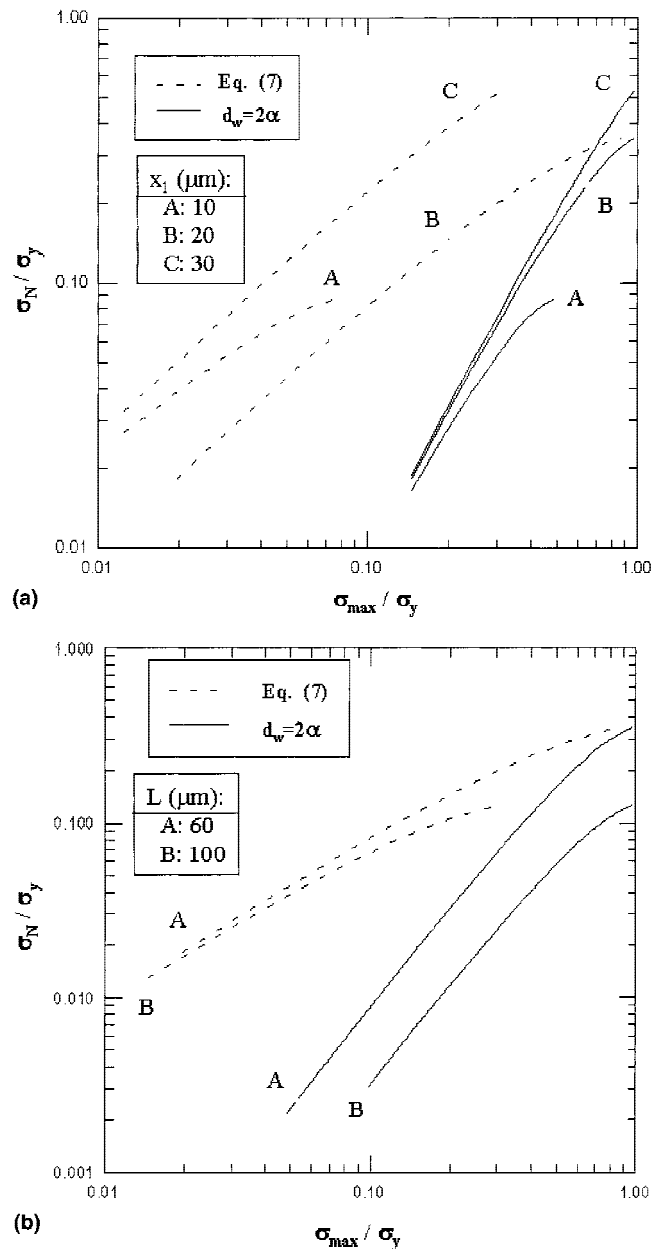

FIG. 7. Effect of surface conditions, (a) asperity spacing and (b) height on the fretting fatigue regimes.

profilometry. (The Ti–6Al–4V specimens were cut out of a forged plate, which had a duplex microstructure, consisting of approximately 50% equiaxed primary alpha phase and approximately 50% of fine lamellar transformed alpha plates. A slight microstructural directionality was present in the longitudinal direction of the plate.) Details of the technique as well as detailed results can be found in Ref. 28. Briefly, it was found that for both the pads and the specimen the asperity height ranged between 0.5 and 1.5 μm, whereas their spacing was between 3 and 10 μm. Thus for the contact area $A = (6.3) \times (6.3)$ mm^2 the total number of asperities in the pad

surface can be given from Eq. (4). However, the number of contacts as defined from Eq. (4) assumes that all asperities in one surface come into contact with all the asperities of the (same area) opposite surface. In addition, Eq. (4) also assumes that the asperities are located on a perfectly flat plane. This second assumption may be true in small scales (i.e., high magnifications), although on a larger scale the wavelet analysis of Frantziskonis *et al.*[19] showed the presence of a periodicity of the surface "structure." This issue is currently being examined in detail; however for the scope of this fretting map development a parameter κ [Eq. (12)] is introduced for determining the actual number of contacts N_{ac}:

$$\kappa = N_{ac}/N \quad . \tag{12}$$

The parameter κ depends upon the large-scale surface periodicity as well as distributions of the asperity heights. For an extremely well-polished specimen with no long range periodicity and a narrow size of asperity height distributions, κ is close to unity; on the other hand for rough specimens containing "deep" machining lines and/ or long range surface roughness periodicities, α drops down to approximately 0.1 or even lower. For the fretting maps of the Ti–6Al–4V alloys presented in the following paragraph, an intermediate κ value of 0.3 was used.

Using the following material, surface, and geometry data, i.e., flow stress σ_y = 930 MPa, elastic modulus E = 115 GPa, asperity spacing λ = 3.5 μm, asperity radius x_1 = 1 μm, half pad length w = 3.15 mm, the fretting map of a Ti–6Al–4V alloy was constructed and is shown in Fig. 8. Because this figure appears to be quite complicated, a step-to-step explanation is attempted. At

first, the solid line represents the boundary between the stick (shaded area) and the mixed regime. Within the mixed regime there are four dashed lines, which correspond to different R ratios. The latter is defined as the length of the stick region to the length of the slip region in the mixed regime. The different R values are presented on the graph and range from R = 1 (stick–mixed regime boundary) to 0.3. In addition, four discrete data points are also shown in the graph. These data (taken from Ref. 27) represent the fretting fatigue life (indicated below each data point) of a Ti–6Al–4V alloy tested at different levels of normal and maximum cyclic stresses. The two solid circles have a fatigue life of an order of magnitude higher than the fretting fatigue life of the open symbols. As indicated in the map, for the data points corresponding to the solid circles the combination of the maximum cyclic and the normal stress is such that the stick regime prevails during the experiments and thus their life reduction due to fretting is minimal. On the other hand, the data points inside the mixed regime have much lower fatigue lives. In fact, in agreement with previous experimental and theoretical results,[7,8] the fatigue life increases as σ_N increases. This can be interpreted by observing that for a constant σ_{max} the R ratio increases with σ_N, implying a wider stick zone and hence a lower stress concentration at the stick-slip boundary.[15]

VI. SUMMARY AND CONCLUSIONS

A methodology for the development of fretting fatigue maps was presented in this article. First, a model based on the cohesion between two contacting surfaces due to an externally applied stress and the subsequent breakup of the cohesion due to an applied cyclic stress on one of the components was developed. The model requires as an input the specimen/pad geometry, as well as several materials parameters, including the surface conditions of the specimen and the fretting pads. Fretting maps, i.e., graphs that allow the determination of the particular fretting fatigue regime as a function of the maximum cyclic stress σ_{max} and the applied normal stress σ_N, were constructed. It was found that the stick regime prevails at low σ_{max} and high σ_N, while the slip regime prevails at high σ_{max} and low σ_N, and the mixed regime occurs at intermediate values of σ_{max} and σ_N. Finally, fretting fatigue data found in the literature were introduced in the fretting maps, which enabled the interpretation of the fretting fatigue life.
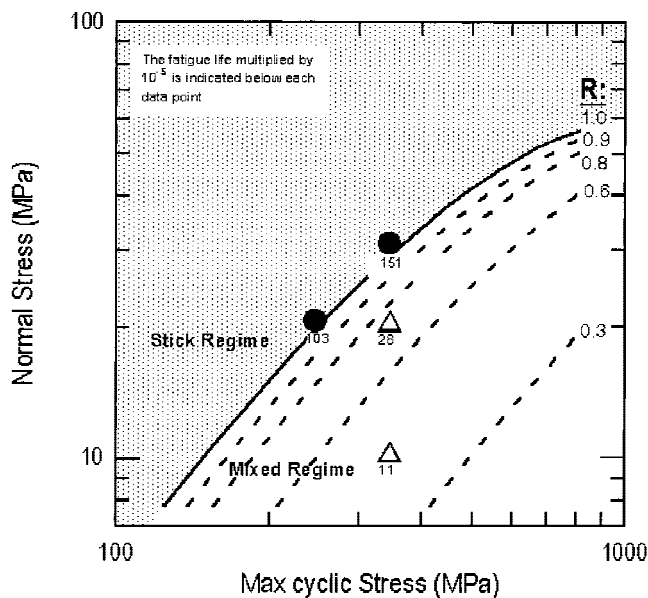

FIG. 8. Fretting map of a Ti–6Al–4V alloy. The individual data points represent experimental data taken from Ref. 27. The dashed lines represent the ratio of the size of the slick zone to the slip zone.

REFERENCES

1. R.B. Waterhouse, Int. Mat. Rev. **37,** 77 (1992).
2. D.A. Hills and D. Nowell, *Mechanics of Fretting Fatigue* (Kluwer Academic Publishers, London, 1994).
3. R.B. Waterhouse, *Fretting Wear: ASM Handbook*, *Vol. 18, Friction, Lubrication, and Wear Technology* (ASM International, Materials Park, OH, 1982).
4. W. Bryggman and S. Sodeberg, Wear, **110,** 1 (1986).
5. D.W. Hoeppner and F.L. Gates, Wear, **70,** 155 (1081).
6. R.B. Waterhouse, *in Specialists Meeting on Fretting in Aircraft Systems* (NATO-AGARD Conference Proceedings, No. 161, 1974), pp. 8.1–8.17.
7. O. Vinssbo and S. Soderberg, Wear, **126,** 131 (1988).
8. C. Petiot, J. Foulquier, B. Journet, and L. Vincent, in *Fretting Fatigue, ESIS 18*, edited by R.B. Waterhouse and T.C. Lindley (Mechanical Engineering Publications, London, 1994) pp. 497–512.
9. R.A. Antoniou and T.C. Radtke, Mater. Sci. Eng. A, **A237,** 229 (1997).
10. K. Nishioka, S. Nishimura, and K. Hirakawa, Bull. JSME, **11,** 437 (1968).
11. K. Nishioka and K. Hirakawa, Bull. JSME, **12,** 692 (1969).
12. D.J. Gaul and D.J. Duquette, Metall. Trans. A, **11A,** 1555 (1980).
13. Z.R. Zhou and L. Vincent, Wear, **181–183,** 531 (1995).
14. S. Fouvry, P. Kapsa, and L. Vincent, Wear, **200,** 186 (1996).
15. K. Nakazawa, M. Sumita, and N. Maruyama, in *Standardization of Fretting Fatigue Test Methods and Equipment*, *STP 119* (American Society for Testing and Materials, Philadelphia, 1992).
16. U. Bryggman and S. Sodeberg, Wear, **125,** 39 (1988).
17. M. Ciavarella, Int. J. Solids Struct., **35,** 2349 (1998).
18. 16. M. Ciavarella, Int. J. Solids Struct., **35,** 2363 (1998).
19. G.N. Frantziskonis, E. Shell, J. Woo, T.E. Matikas, and P.D. Nicolaou, in *SPIE Conference on Nondestructive Evaluation of Aging Materials and Composites III,* SPIE Vol. 3585, edited by G.Y. Baaklini, C.A. Lebowitz, and E.S. Boltz (SPIE, Newport Beach, CA, 1999), pp. 11–27.
20. A.L. Hutson, T. Nicholas, and R. Goodman, in *Proccedings of the 3rd National Turbine Engine High Cycle Fatigue Conference, San Antonio, TX, February 2–5, 1998.*
21. M.P. Szolwininski and T.N. Farris, Wear, **198,** 93 (1996).
22. W.A. Backofen, *Deformation Processing* (Addison-Wesley, Reading, MA, 1972).
23. D.S. Wilkinson, Ph.D. Thesis, Cambridge University, Cambridge, United Kingdom, 1978.
24. A.D. Sarkar, *Wear of Metals* (Pergamon Press, New York, 1976).
25. T.E. Matikas, in *Proceedings of the 3rd National Turbine Engine High Cycle Fatigue Conference, San Antonio, TX, February 2–5, 1998*, pp. 29–46.
26. J. Foulquier and C. Petiot, *Fretting-Fatigue Behavior of Major Helicopter Alloys and Influence of Surface Protections* (Aerospatiale, Louis Bleriot Research Center, France, unpublished research).
27. C. Lutynski, G. Simansky, and A.J. McEvily, *ASTM STP 780* (American Society for Testing and Materials, Philadelphia, 1982), pp. 150–164.
28. P.D. Nicolaou, T.E. Matikas, and E.B. Shell, in *SPIE Conference on Nondestructive Evaluation of Aging Materials and Composites III*, edited by G.Y. Baaklini, C.A. Lebowitz, and E.S. Boltz (SPIE, Newport Beach, CA, 1999), Vol. 3585, pp. 28–39.